

Ritchey–Common test for a 1.5 m-diameter flat mirror

S. Zhu

zhangxiaohui123@163.com

X. H. Zhang

Changchun Institute of Optics, Fine Mechanics and Physics, Chinese Academy of Sciences, Changchun 130033, China

Changchun Institute of Optics, Fine Mechanics and Physics, Chinese Academy of Sciences, Changchun 130033, China

This study intensively investigates the Ritchey–Common test to enable high-precision measurement of a plane mirror figure with a diameter of 1.5 m. We present a method for separating the adjustment error combined with tested data and the least-square method. We also use the transformation relationship of coordinates and amplitude between the test system pupil plane and the flat mirror to calculate the flat mirror surface error. Ritchey–Common test is conducted on a 100 mm-diameter plane mirror. Results prove that the algorithm can effectively isolate the adjusting-error effect. Compared with the direct test results from interferometer, the RMS calculation accuracy of the algorithm is better than $\lambda/100$ ($\lambda = 0.6328 \mu\text{m}$). Accordingly, we build a Ritchey–Common test light path for the 1.5 m plane mirror. After analyzing the factors affecting the experiment results, we obtain the surface PV value of 0.391λ and RMS of 0.0181λ . Finally the test achieves full aperture detection for a large-diameter plane mirror surface.

[DOI: <http://dx.doi.org/10.2971/jeos.2014.14053>]

Keywords: Ritchey–Common, surface, flat, optical, interference

1 INTRODUCTION

The problem of measuring a large-diameter mirror surface in high precision has not been properly solved because of the limitations of test equipment and conditions [1, 2]. Ritchey–Common test is an effective way to test a plane mirror surface with a large diameter [3]. Compared with a large caliber interferometer, a high-precision spherical mirror, which is 1.3 times greater in diameter than the flat mirror being tested as a reference mirror, is easy to fabricate. The testing process is relatively stable and can detect large-diameter mirrors with the use of a small caliber interferometer [4]–[7].

The present study intensively investigates the Ritchey–Common test. We analyzed the transformation relationship between the system wavefront aberration and surface error of the plane mirror that was tested, and built a theoretical model of the algorithm. The experiment was conducted on a small-caliber plane mirror, which proves that the algorithm can effectively isolate the adjusting-error effect and achieve high-precision measurement. Ritchey–Common test light path was set up to test a plane mirror with a diameter of 1.5 m. The measurement of the 1.5 m plane mirror surface was achieved using the two-angle test.

2 RITCHEY–COMMON TEST PRINCIPLE

Figure 1 is schematic diagram of the Ritchey–Common test. The collimated light beam from the interferometer goes through a standard lens and is emitted in the form of a spherical wave [8]–[10]. The focus of the lens coincides with the curvature center of standard spherical mirror. The flat mirror was inserted into the divergent light path with a certain Ritchey angle (the angle between the divergent beam

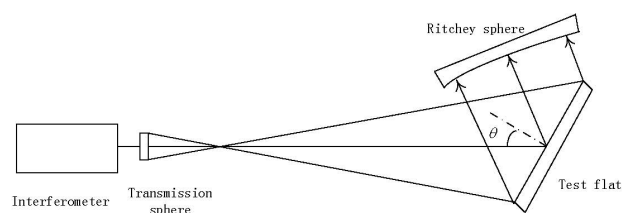


FIG. 1 Ritchey–Common test setup.

axis and the normal of the flat mirror). The test beam incident on the flat mirror, and then the standard flat mirror and standard spherical mirror reflected the beam. Beams that return along the light paths interfere with the reference beam inside the interferometer. Finally we calculated the flat mirror surface error based on the measured wavefront data [11].

In the Ritchey–Common test, image compression that was presented on the spot on the pupil plane in the sagittal direction, which approximately has an elliptical shape, because beams touch flat mirrors with a certain Ritchey angle. This condition complicates the transformation relationship between the system wavefront aberration and mirror surface error in the present study [12, 13]. One is the coordinate transformation from pupil plane to mirror surface, whereas the other one is a different transformation relationship from different sampling points that different incident angles cause. As shown in Figure 2, the test surface and pupil plane coordinate systems are established [14]. x_s, y_s represents the flat surface coordinate and x_p, y_p represents the pupil coordinate. The coordinate transformation relationship between test flat and pupil plane coordinate systems is obtained using a geo-

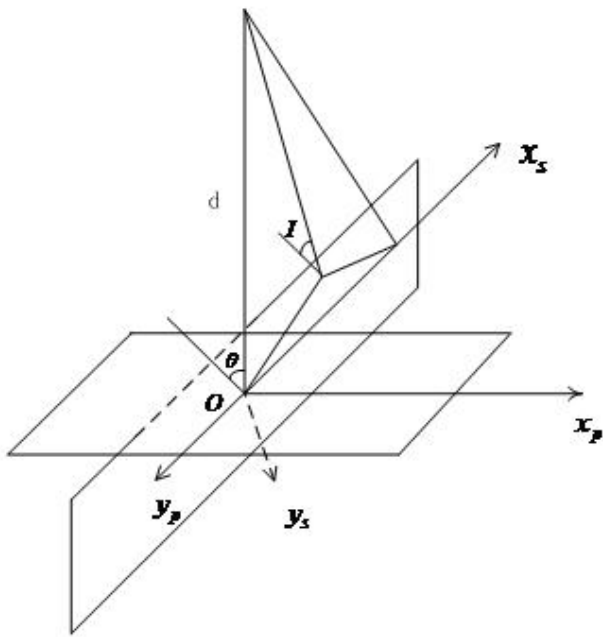


FIG. 2 Relation between pupil coordinate and flat coordinate.

metrical formula:

$$x_s = \frac{d \cdot x_p}{d \cdot \cos \theta - x_p \cdot \sin \theta} \tag{1}$$

$$y_s = \frac{y_p \cdot (d + x_s \cdot \sin \theta)}{d}, \tag{2}$$

where d represents the distance from the focal point of the interferometer lens to the center of the flat mirror. In the diverging path that the optical axis obliquely touches, the incident angle at each point on the flat mirror is different. The arbitrary incidence angle can be represented as an expression of a Ritchey angle based on the position relationship between each point and the main optical axis:

$$\cos \varphi = \frac{d \cos \theta - x_s \sin \theta}{\sqrt{d^2 + x_p^2 + y_p^2}}. \tag{3}$$

The flat mirror was inserted into light paths with a certain Ritchey angle θ , a system wavefront aberration $W(x_p, y_p)$ is changed with changing the flat mirror surface error $S(x_s, y_s)$. After two reflections, the relationship between these two is as follows:

$$S(x_s, y_s) = T \left[\frac{W(x_p, y_p)}{4 \cdot \cos \varphi} \right], \tag{4}$$

where $T[\bullet]$ represents the operator that flat coordinate (x_s, y_s) mapped from the pupil coordinate (x_p, y_p) using Eqs. (1) and (2).

The principle of Ritchey–Common test is simple. However, some difficulties must be addressed. Adjusting the light path during testing will introduce constant error, tilt error, and defocus error. The flat mirror was inserted into a light path at an angle, which made the measured wavefront data contain not only astigmatism, which is inherent in the plane mirror, but also the effect that the large curvature radius caused. We

cannot obtain the exact surface of the flat mirror through a single test, thus more than one test needed. Two common methods that we use for testing are to change Ritchey angle or rotate around the normal of the flat mirror. Based on the existing laboratory test conditions, we changed the Ritchey angle to separate the adjustment error through the processes of the two–angle test.

The effects that the constant term and tilt term in the adjustment error have on test results are usually negligible, thus we concentrate more on the effects that the defocus term error cause. The system wavefront data that were tested two times are recovered through coordinate mapping and amplitude transform. The results of the tested surface are $S_1(x_s, y_s)$ and $S_2(x_s, y_s)$ in the flat coordinate system. The two results contain effects from the adjustment error. Assume $S_0(x_s, y_s)$ is the real surface of the flat mirror, the results of surface figure are:

$$S_1(x_s, y_s) = S_0(x_s, y_s) + a_1 \cdot D_1(x_s, y_s), \tag{5}$$

$$S_2(x_s, y_s) = S_0(x_s, y_s) + a_2 \cdot D_2(x_s, y_s). \tag{6}$$

a_1, a_2 represents the coefficient of the defocus term error, which the system adjustment introduces during the two–angle test. D_1, D_2 represents the surface error that the flat coordinate mapped from the Zernike polynomial defocus term in pupil coordinates at different test angles. We can obtain an independent system error polynomial with an exact surface using Eqs. (5) and (6):

$$\Delta S = S_1 - S_2 = a_1 \cdot D_1 - a_2 \cdot D_2 = a \cdot D \tag{7}$$

We solve the system error coefficient a to fit all the valid data points of the full aperture in Eq. (7) combined with the least square methods. The optimal solution S_0^* is solved in the two–angle test to substitute the coefficient a into Eq. (5) or (6).

3 VERIFICATION EXPERIMENT FOR ALGORITHM ACCURACY

To verify that the algorithm can achieve a high–precision measurement in the Ritchey–Common test, and the effects of the adjustment error in the test are separated to make the flat mirror figure error more accurate. The test is conducted on a plane mirror with a diameter of 100 mm. We choose a spherical mirror with a diameter of 280 mm and a curvature radius of 1172 mm as the standard mirror. The test platform is shown in Figure 3. The interferometer lens and standard spherical mirror must be calibrated in advance, and the effect is compensated as the system mirror. The state that the flat mirror presents in the meridian direction does not change as the flat mirror is rotated to change the Ritchey angle.

The effect on the final test result is negligible because the standard lens of the commercial interferometer currently has high precision. The standard spherical mirror is tested and the surface figure is shown in Figure 4, and the accuracy meets requirements of the Ritchey–Common test. Then, the Ritchey–Common test light path is built. In order to verify the theoretical analysis we selected three angles, 24.8°, 40.3°, and 53.1°

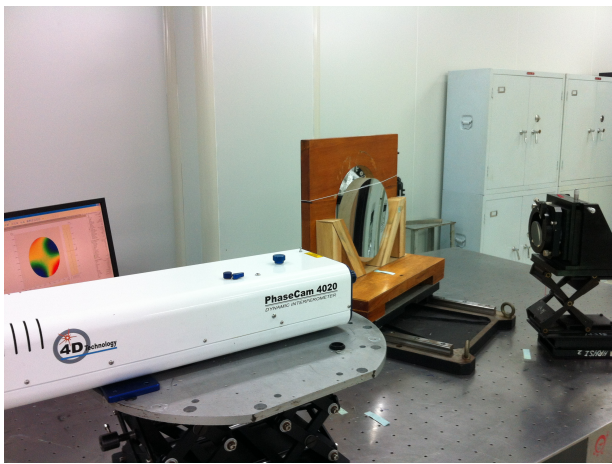


FIG. 3 R-C test set-up.

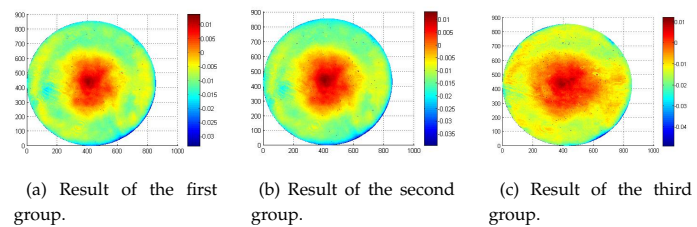


FIG. 5 Result of the three groups.

	PV(λ)	RMS (λ)
Result of the first group	0.149	0.0177
Result of the second group	0.166	0.0221
Result of the third group	0.197	0.0209

TABLE 2 Result of the three groups.

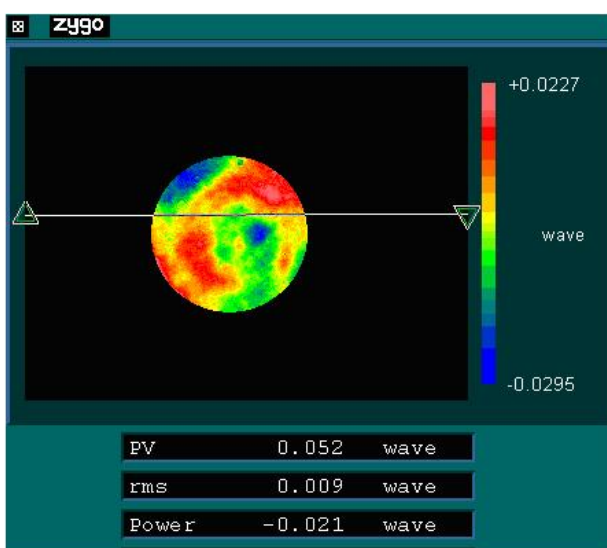


FIG. 4 Reference sphere surface.

for the test. Ritchey angle can be calculated using the image compression ratio in the pupil plane of the test system. The calculation accuracy can be controlled within 0.2° .

The system wavefront error is measured in each Ritchey angle. The built-up sequence of three wavefront error groups are divided into pairs, which are $[24.8^\circ, 40.3^\circ]$, $[24.8^\circ, 53.1^\circ]$, and $[40.3^\circ, 53.1^\circ]$, to analyze and recover three groups of wavefront error using the Ritchey-Common test algorithm, then interpolate and fit the surface figure of the test flat mirror using coordinate mapping and amplitude transform. The defocus coefficient is isolated to separate the errors of the three data groups using the least square methods combined with theoretical analysis, as shown in Table 1.

The flat mirror surface figure, which interpolating and fitting made, removes the effects that the system adjustment error and standard spherical mirror surface error caused. Finally, we obtain the surface figures of the three flat mirror groups through fitting, as shown in Figure 5.

Specific information of each surface figure group is listed in Table 2:

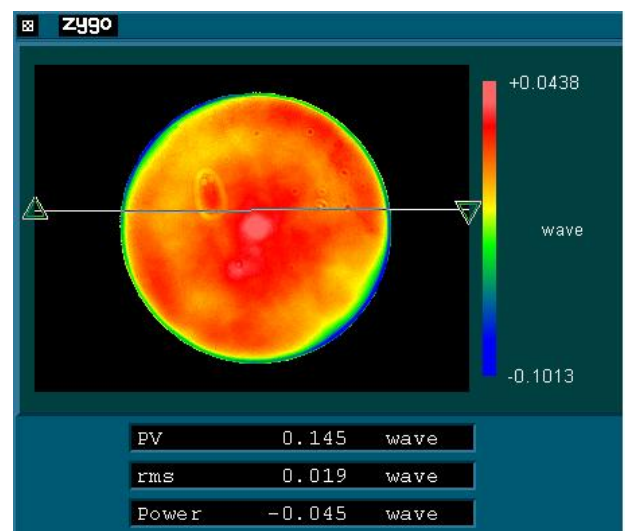


FIG. 6 Result of interferometer.

We use a Zygo interferometer to directly test the surface figure of the flat mirror whether or not the accuracy of the final results meets the requirements. The results are shown in Figure 6. The value of surface error PV is 0.145λ ($\lambda = 0.6328 \mu\text{m}$), and RMS is 0.019λ ($\lambda = 0.6328 \mu\text{m}$).

The experimental results show that compared with the interferometer test results, RMS residuals had relative results of 0.0013λ , 0.0031λ , and 0.0019λ . The calculation accuracy of PV values can be controlled within 0.1λ , and RMS values can be controlled within 0.01λ using this method, which can achieve the Ritchey-Common test requirements of high precision.

From the three data groups listed in Table 1, this method, which separates the system adjustment error combined with the least-square method, can calculate the coefficient of the adjustment error term effectively. After removing the adjustment error effects, good uniformity can be found when the three groups of results are compared. After analyzing the errors of three RMS value groups, the average value of RMS is found to be 0.0202λ and the RMS error is 0.0022λ . This method can guarantee the stability of the test results and meet the accuracy requirements, while verifying the effectiveness and correctness of the algorithm.

First group	Coefficient of defocus (μm)	Second group	Coefficient of defocus (μm)	Third group	Coefficient of defocus (μm)
24.8°	0.0154	24.8°	0.0219	40.3°	0.0255
40.3°	0.0179	53.1°	0.0306	53.1°	0.0310

TABLE 1 Coefficient of defocus solved using the least-square method.

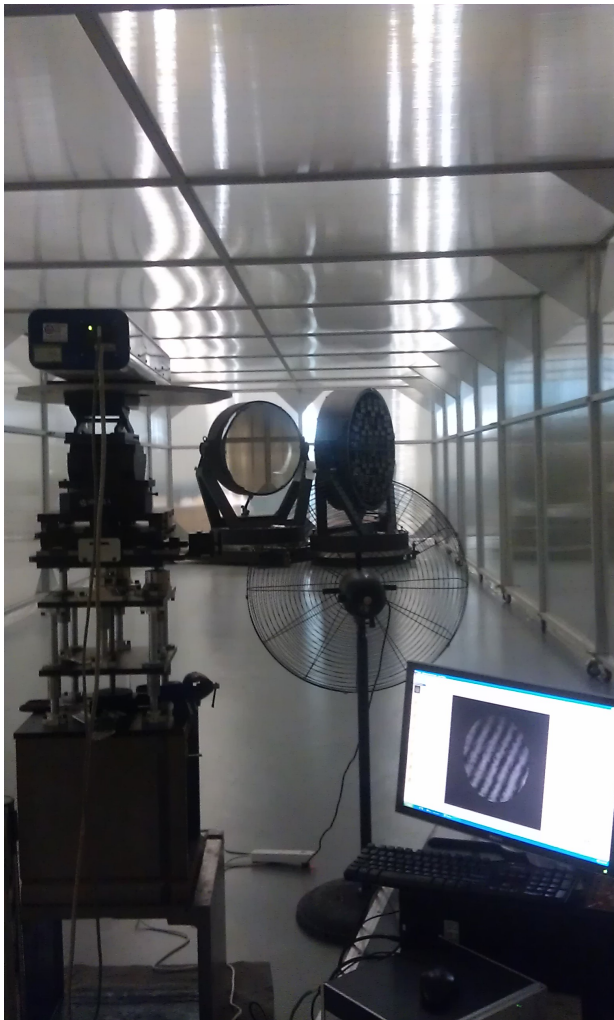


FIG. 7 Experimental layout.

4 SURFACE FIGURE TEST OF A FLAT MIRROR WITH A DIAMETER OF A 1.5 M

4.1 Experiment

On the basis of the above analysis, the surface figure of a flat mirror with a diameter of 1.5 m is tested using the Ritchey–Common test with a standard spherical mirror that has a diameter of 1.8 m and a curvature radius of 15 m. The 4D dynamic interferometer, which has a good seismic performance, is selected to reduce the vibration effects. The test system is composed of an interferometer, interferometer spherical lens, a measured spherical mirror, and a standard reflector. The test light path is shown in Figure 7. We select the two Ritchey angles of 32.3° and 45.6° and a test distance of 13 m are selected for the experiment.

First, we calibrate the selected standard spherical mirror to

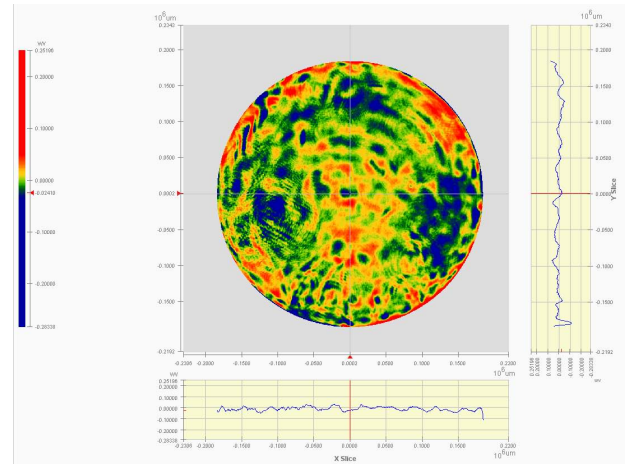


FIG. 8 Reference sphere surface condition PV=0.215 λ , RMS=0.0197 λ .

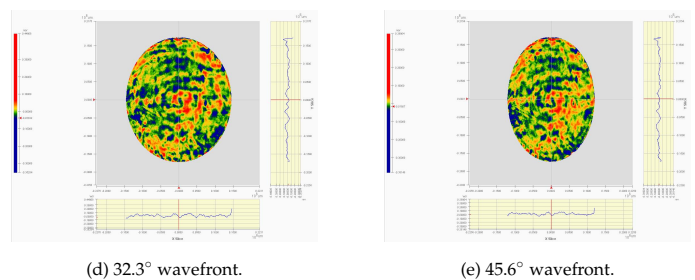


FIG. 9 Wavefront of two R-C angles.

ensure that the surface error accuracy meets the test requirements. The surface figure is shown in Figure 8. Second, the Ritchey–Common test light path is built. Ensuring that the standard lens of the interferometer, the measured flat mirror, and the standard spherical mirror has a center alignment is important when building the light path for the Ritchey angle to become accurate. Third, the test is conducted for the second time after the Ritchey angle is changed. Maintaining the distance from the focus of the interferometer standard lens to the center of flat mirror is important to ensure the uniformity and accuracy of coordinate mapping in the two-angle test. The light path is modified until the measured wavefront aberration is stable, then the wavefront data is tested and recorded.

4.2 Experimental results

The wavefront in two Ritchey angles is shown in Figure 9. Wavefront aberration is analyzed and recovered using the aforementioned method, then tested flat mirror surface figure is obtained through interpolation and fitting of the coordinate mapping and amplitude transformation.

The least-square method is used on two data groups to achieve error separation combined with theoretical analysis,

Ritchey angle	Coefficients (μm)
32.3°	0.0095
45.6°	0.0085

TABLE 3 Coefficient of defocus.

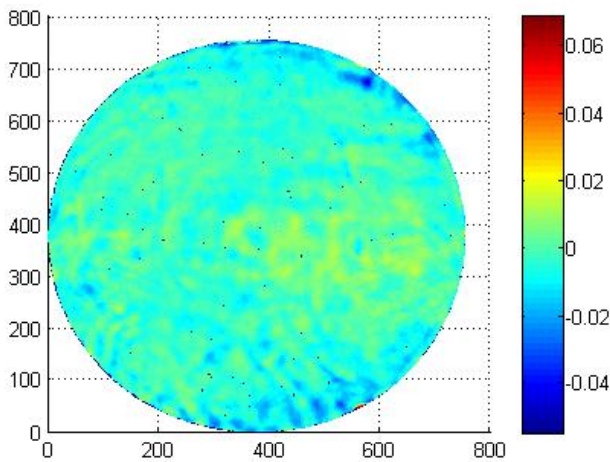


FIG. 10 Surface of a flat mirror with a diameter of 1.5 m.

and isolated defocus coefficient, as shown in Table 3. After removing the adjustment error and spherical mirror surface error from the results, the flat mirror surface figure is finally obtained through calculation. As shown in Figure 9, the value of surface PV is 0.391λ , and RMS is 0.0181λ .

The Ritchey angle is solved through image compression ratio in the pupil plane. The calculation accuracy is better than 0.2° . The accuracy of test results can be guaranteed when the measuring error of the Ritchey angle is smaller than 1° . The distance length is 13 m, which is obtained with the use of the high-precision diastimeter through averaging the testing values of repeated measurements. The allowed band of measuring error is from -20 mm to 20 mm, which also meets the accuracy requirements.

In summary, we conducted the surface figure test on a flat mirror with a diameter of 1.5 m, and analyzed the effects that the Ritchey angle caused, and tested distance or other factors. However, some problems must still be solved. For example, the axes of the standard lens of an interferometer, the measured flat mirror, and the standard spherical mirror do not coincide, which causes coordinate and amplitude mapping errors. Ensuring that the state flat mirror presents in the meridian direction is difficult because of the mechanism alignment limitations when changing the Ritchey angle in the two-angle test. The experimental environment factor has a large effect on test stability. All of these factors can introduce error to the test results and needs further analysis and study.

5 CONCLUSION

The present study intensively investigates Ritchey-Common test to achieve a high-precision measurement for a flat mirror figure with a diameter of 1.5 m. We present the method of separating the adjustment error combined with data from a two-

angle test and least-square method. We also use the transformation relationship of coordinate and amplitude between a test system pupil plane and the flat mirror to calculate the flat mirror surface error. The accuracy and validity of the solution is verified through conducting the Ritchey-Common test on a small-caliber flat mirror with a given calculation accuracy for the algorithm. Finally, we build a Ritchey-Common test light path to test the flat mirror with a diameter of 1.5 m. From the two-angle test data, we obtain the value of surface PV, which is 0.391λ , and RMS is 0.0181λ . The results achieve full aperture detection for a large-diameter plane mirror surface, and set the foundation for more large-caliber flat surface tests in the future.

References

- [1] J. E. Yellowhair, *Advanced technologies for fabrication and test of large flat mirrors* (Ph.D. Dissertation, University of Arizona, Tucson, 2007).
- [2] L. B. Yu, E. Barakat, T. Sfez, L. Hvozdar, J. Di Francesco, and H. Peter Herzig, "Manipulating Bloch surface waves in 2D: a platform concept-based flat lens," *Light Sci. Appl.* **3**, e124 (2014).
- [3] S. Zhu, and X. H. Zhang, "Application of error detach technology in Ritchey-Common test for flat mirror," *Opt. Precision Eng.* **22**, 7-12 (2014).
- [4] M. S. Bai, P. Li, J. K. Zhang, and L. Teng, "Improvement on nonuniformity for sphere mirrors with large radius of curvature," *Opt. Precision Eng.* **21**, 554-560 (2013).
- [5] H. Ren, L. Ma, X. Liu, Y. He, W. G. Wan, and R. H. Zhu, "Optical element test with multiple surface interference," *Opt. Precision Eng.* **19**, 1144-1150 (2013).
- [6] X. F. Fan, W. T. Zheng, and D. J. Singh, "Light scattering and surface plasmons on small spherical particles," *Light Sci. Appl.* **3**, e179, 1-14 (2014).
- [7] P. Girshovitz, and N. T. Shaked, "Doubling the field of view in off-axis low-coherence interferometric imaging," *Light Sci. Appl.* **3**, e151, 1-9 (2014).
- [8] D. Malacala, *Optical Shop Testing* (Wiley, New York, 2007).
- [9] Z. H. Tian, Z. G. Shi, W. Q. Liu, H. J. Yang, and Y. X. Sui, "High-accuracy measurement for radius of curvature and its uncertainties," *Opt. Precision Eng.* **21**, 2496-2501 (2013).
- [10] J. Liu, E. L. Miao, Y. Qi, Y. X. Sui, and H. J. Yang, "Measurement of optical surface based on intensity self-calibration phase-shift algorithm," *Opt. Precision Eng.* **22**, 2008-2013 (2014).
- [11] K. L. Shu, "Ray-trace analysis and data reduction methods for the Ritchey-Common test," *Appl. Optics* **22**, (12), 1879-1886 (1983).
- [12] S. Han, E. Novak, and M. Schurig, "Application of Ritchey-Common test in large flat measurements," *Proc. SPIE* **4399**, 131-136 (2001).
- [13] S. Han, E. Novak, and M. Schuring, "Ritchey-Common Test used for Measurement of Astronomical Optic," *Proc. SPIE* **4842**, 270-273 (2003).
- [14] ZYGO Corporation, *Ritchey-Common Metro-Pro Application [M]*, (ZYGO Corporation, Connecticut, 2004).
- [15] S. Zhu, and X. H. Zhang, "Eliminating alignment error and analyzing Ritchey angle accuracy in Ritchey-Common test," *Opt. Commun.* **311**, 368-374 (2013).